JOURNAL OF CATALYSIS 91, 185–196 (1985)

Mössbauer Spectroscopy Observations of Local Temperature Rises in a Silica-Supported Iron Catalyst

R. J. MATYI,[1] J. B. BUTT,* AND L. H. SCHWARTZ†

†*Department of Materials Science and Engineering and* **Department of Chemical Engineering, Ipatieff Laboratory, Northwestern University, Evanston, Illinois 60201*

Received May 11, 1984; revised September 21, 1984

Mössbauer spectroscopy has been used to observe the local (or microscopic) temperature of a silica-supported iron catalyst used in the Fischer–Tropsch synthesis reaction. The internal magnetic field of the iron carbide crystallites, measured while the catalyst was situated in an *in-situ* cell, was used to measure temperature of the crystallites under reaction conditions. At nominal bulk temperatures of 275 and 300°C, temperature rises of 13 and 19°C were recorded when the gas flow to the catalyst was changed from helium to the $3H_2/CO$ reaction mixture. These local temperature rises of the supported crystallites were in contrast to observed decreases in the bulk catalyst temperature when the reaction mixture was introduced. The iron carbide crystallites transformed from the ε' phase to the more stable χ-carbide after prolonged treatment in helium.

I. INTRODUCTION

It has long been known that if a catalytic reaction is highly exothermic the heat generated by the reaction may not be dissipated at a rapid enough rate to maintain isothermal conditions. This problem can be severe in reactions conducted under industrial conditions where the catalyst may be in the form of a compressed pellet and high conversions to products are required for economic feasability. Under these conditions the limitations to mass and heat transfer that exist within the catalyst pellet can cause the establishment of large intrapellet temperature gradients. Several analytical treatments such as the original expression derived by Damköhler (cited in (*1*)) have predicted that the magnitude of the temperature gradient for an exothermic reaction can be as large as several hundreds of degrees. A number of experimental investigations (*2–4*) have monitored the temperature profile within a pellet using embedded thermocouples and have confirmed the existence of significant thermal gradients.

However, the above studies have been concerned with macroscopic temperatures; that is, the catalyst pellet is assumed to have a pseudo-homogeneous structure, thus allowing the application of continuum heat and mass transfer equations to essentially a bulk material. The fine structure of the catalyst (metal crystallites situated on an inert support) is neglected. While this treatment may be adequate for engineering applications and reactor design, it circumvents the basic question of what is the true temperature that a reactant molecule experiences as it approaches a catalytically active surface. When a molecule reacts on the surface of a supported metal crystallite, the heat evolved may or may not be dissipated before the next molecule comes into the vicinity of the surface. It is thus easy to visualize a situation where the bulk temperature of the catalyst (macroscopic particles and surrounding gas) would differ from the local temperature at the surface of a small metal crystallite.

Consideration of this problem is a topic

[1] Present address: Texas Instruments Incorporated, Dallas, Texas 75265.

0021-9517/85 $3.00

that has appeared periodically in the reaction engineering literature over a number of years. For example, Luss (*5*) considered the local temperature rise that would be expected when crystallites of different geometries were attached to constant temperature supports and subsequently exposed to reactive atmospheres and the temperature fluctuations associated with exothermic reactions. Luss showed that, for exothermic reactions, the temperature differential between the crystal and the support, calculated using the conventional Fourier heat transfer equation, could be as large as several hundred degrees in excess of the ambient temperature. The magnitude of the local temperature rise was found to be strongly dependent on the size and geometry of the metal crystals, as well as the length of time during which the reacting molecule releases heat into the crystal. Chan *et al.* (*6*) refined Luss' treatment by including the finite speed of heat propagation within the metal crystallite; their numerical results were in qualitative agreement though larger in magnitude than those predicted by Luss. Ruckenstein and Petty (*7*) have pointed out, however, that a classical diffusion equation is only valid if the initial input is permitted to propagate through a large enough distance for a sufficiently long time. They showed that as the propagation speed of the exothermic heat pulse decreased, the surface region of the crystallite would become hotter and would cool down more slowly than predicted from Luss' model.

An alternative approach to the question of heat dissipation in supported crystallites has been taken by Steinbrüchel and Schmidt (*8*). Rather than use a modification of a continuum approach, Steinbrüchel and Schmidt considered the creation and interactions of phonons in a metal crystallite. They found that a phonon treatment led to higher predicted temperature differentials than were calculated from the continuum approach. Moreover, Steinbrüchel and Schmidt observed a much slower decay in the local temperature after the reaction and a dependence on crystallite size that differed substantially from that predicted by Luss and Chan *et al.*

Recently, Holstein and Boudart (*9*) have developed an alternative model for the calculation of the temperature difference between a supported catalyst particle and its support. In contrast with the conclusions of the investigations described earlier, Holstein and Boudart calculated that the maximum temperature difference between a catalyst particle and its support would be less than 0.03% under normal reaction conditions. It should be noted that the upper limit of the temperature difference obtained from this model was calculated using macroscopic heat transfer relationships.

No matter which of the above treatments is more realistic, it is clear that the existence of a local temperature rise in a supported metal catalyst would have serious implications. If the predictions documented above are correct, then it is possible that the temperature that a reactant molecule experiences as it approaches an active surface is different from the temperature recorded by a thermocouple in the reactor. A large body of reaction rate data obtained from supported catalysts might therefore be suspect. In addition, the existence of a local temperature rise would have implications in the study of oscillatory behavior of catalysts. Several investigations (*10–12*) of oscillations in the reaction rate of catalytic reactions have suggested the existence of a catalyst surface temperature that is different from the ambient temperature.

Few experimental studies of the existence of a local temperature rise in supported metal catalysts have been published in the literature. Cusamano and Low (*13*) used an infrared radiometric technique to examine the adsorption of oxygen on several silica-supported nickel catalysts. An increase in radiometric emission was observed when oxygen was pulsed over the reduced catalyst that corresponded to temperature increases ranging from 137 to 215°C. More recently, Kember and Shep-

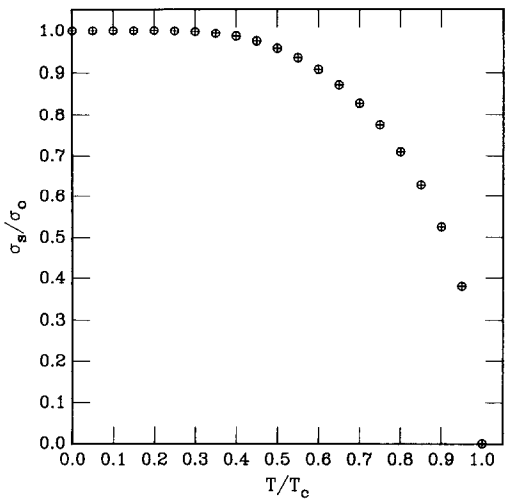

FIG. 1. Dependence of reduced saturation magnetization σ_s/σ_0 on reduced temperature T/T_c. Points calculated from Eq. (1).

pard (*14*) recorded the infrared emission from a 13% palladium on silica gel catalyst during the oxidation of CO. Kember and Sheppard reported an estimated temperature increase of 190°C during the oxidation reaction when the nominal temperature of the reactor was at 300°C.

Mössbauer spectroscopy, a tool that has been used extensively for the characterization of iron catalysts (*15, 16*), possesses certain characteristics that make it an attractive candidate for temperature measurements of supported metal crystallites. In particular, the Mössbauer spectrum of iron compounds is highly sensitive to the magnetic environment of the absorbing material. The positions of the absorption peaks in a magnetically ordered material (such as the iron carbide catalysts that result in the Fischer–Tropsch synthesis reaction) are proportional to the magnitude of the magnetic field at the nucleus of the absorbing atom. Preston *et al.* (*17*) have studied the temperature dependence of the internal magnetic field of natural iron, and they found that the decrease in the field strength with increasing temperature followed the Brillouin function dependence of the saturation magnetization (*18*). This dependence, shown in Fig. 1, is given by

$$\frac{\sigma_s}{\sigma_0} = \tanh \frac{\sigma_s/\sigma_0}{T/T_c}, \qquad (1)$$

where T/T_c is the ratio of the actual temperature to the Curie temperature, and σ_s and σ_0 are the internal magnetic field strengths at temperatures T and 0°K, respectively.

It is therefore likely that the internal magnetic field of an iron catalyst can be used as an "internal thermometer." It has been shown (*15, 16*) that ε'-iron carbide is formed during the Fischer–Tropsch reaction over supported iron; the Curie temperature of this carbide has been reported (*19*) to be approximately 450°C. Since the Fischer–Tropsch synthesis occurs around 250–300°C, the corresponding value of the reduced temperature T/T_c is about 0.8. Reference to Fig. 1 shows that the temperature used at reaction conditions is in the region where a small change in temperature would cause a large change in the internal magnetic field of the iron carbide. By monitoring the magnitude of the magnetic field during reaction conditions (accomplished by measuring the splitting of the absorption lines in the Mössbauer spectrum) it is possible to determine the temperature of the iron carbide crystallites independent of the ambient thermal conditions.

II. EXPERIMENTAL

The iron catalyst used in this study was prepared by impregnating Cab-O-Sil EH5 silica gel with an aqueous solution of iron nitrate in water. The details of the preparation procedure, which have been reported elsewhere (*20*), were similar to those employed by Raupp and Delgass (*16*). Calcination was carried out in an atmosphere of 1% O_2/99% He in a fluidized bed reactor at 450°C for 24 h. The supported iron oxide contained approximately 19% iron metal by weight as calculated from the amount of iron nitrate consumed during impregnation. The iron loading was confirmed by X-ray analysis performed with a Cambridge S4

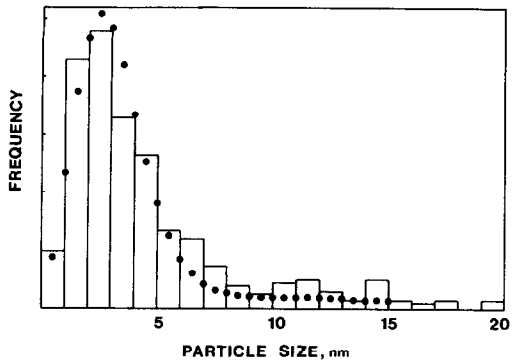

FIG. 2. Particle size distribution of reduced iron metal crystallites determined from X-ray line broadening analysis and dark-field transmission electron microscopy. Solid points = X-ray data; open bars = TEM data.

scanning electron microscope equipped with an EDAX X-ray analyzer.

The average particle sizes and particle size distributions of the calcined oxide precursor, the reduced iron metal and the iron carbide crystallites were measured using X-ray diffraction line broadening analysis (XRD), dark-field transmission electron microscopy (TEM), and small-angle X-ray scattering (SAXS). The supported oxide crystallites exhibited a broad particle size distribution, and the distribution curves obtained from TEM and the Fourier analysis of the oxide diffraction profiles agreed well with each other. The number-average particle size of the oxide crystallites measured by electron microscopy was 10.3 nm, while the Warren–Averbach treatment (*21*) of the Fourier analysis yielded an average crystallite size of 9.3 nm. The total surface area of the oxide crystallites determined with SAXS using the method of Goodisman *et al.* (*22*) was in agreement with the results of the Fourier analysis and TEM.

The size distribution of the reduced metal crystallites was much different from that of the oxide. Both TEM and X-ray line broadening analysis showed a distribution curve with a peak around 3 nm and a long tail extending beyond 15 nm. This particle size distribution, shown in Fig. 2, yielded a TEM number-average particle size of 5.0 nm. The size distribution of the supported iron carbide was measured by TEM and found to be very similar to that of the reduced metal. Unfortunately, overlapping diffraction peaks prevented X-ray line broadening analysis of the carbide. The surface area from SAXS agreed with the TEM data from both the reduced metal and the carbide. The TEM particle size of the carbide was determined to be 5.2 nm.

Reduction and carburization of the oxide precursor were performed in the Mössbauer *in-situ* reactor cell illustrated in Fig. 3. The cell consisted of a copper block with a $\frac{1}{2}$-in. aperture for γ-ray transmission. The initial oxide catalyst sample, placed in the aperture between the gas inlet and outlet ports, was in the form of a self-supporting wafer that had been compressed at 8000 lbs pressure. The cell was sealed on both sides by a $\frac{1}{8}$-in. beryllium window with a 0.006-in. copper foil gasket. A gas-tight seal was effected by compressing the beryllium win-

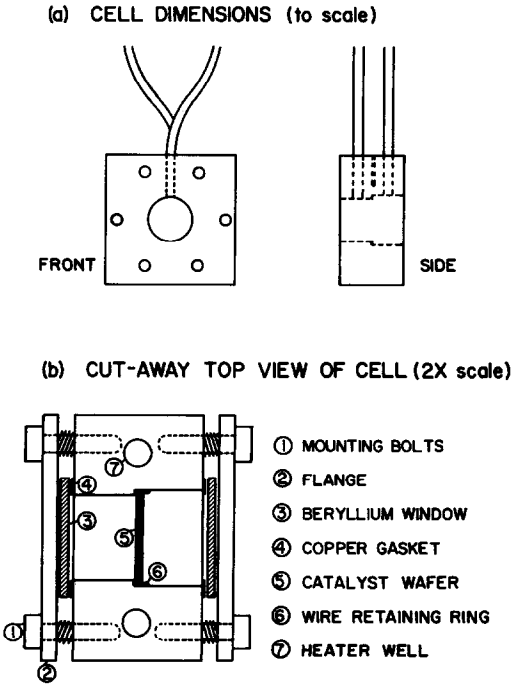

FIG. 3. Schematic of Mössbauer *in-situ* reactor cell.

dow against the gasket with a flange bolted to the cell body.

The cell was heated by two 150-W cartridge heaters (Watlow Firerod) connected in parallel. The signal to the cell temperature controller (Theal TCD-1200) was generated by an ungrounded thermocouple situated in a well at the top of the copper block. In addition, the temperature of the catalyst wafer itself was monitored by a thermocouple routed down the gas inlet line. It was found that at steady state the temperature of the wafer fluctuated by less than 0.25°C.

Reduction and carburization of the oxide precursor were accomplished using a gas handling system described elsewhere (*20*). The gases used were helium (99.995% minimum purity), hydrogen (99.99%), and a mixture of 25.2% CO (99.3%) in hydrogen (99.999%). The $3H_2/CO$ reaction mixture was contained in a glass-lined aluminum tank in order to eliminate the formation of iron carbonyls. A silica gel trap, maintained at a temperature of −78°C by a bath of dry ice and acetone, removed water and other condensables from the gas stream. Removal of oxygen was accomplished by a trap consisting of 15% manganese oxide on silica gel. During normal operations the reaction cell was flushed with helium prior to heating to a controlling temperature of 410°C. The gas flow was then switched to hydrogen and the catalyst was reduced to the metallic state for 24 h. After reduction, the cell was cooled to 250°C under flowing hydrogen. Carburization of the iron catalyst was accomplished by changing the gas flow to the $3H_2/CO$ reaction mixture. The catalyst was fully transformed from the metallic state to the carbide within 2 h; this is in agreement with other investigations of silica-supported iron catalysts (*15, 16*). Upon the completion of carburization, the temperature was raised to the desired level and the Mössbauer spectrum was recorded under reaction conditions. A typical spectrum required data acquisition times of 2 to 3 h. Corresponding spectra under nonreaction conditions were then obtained under flowing helium after the cell had been flushed with helium for 15–20 min.

The *in-situ* Mössbauer data were collected using an Austin Scientific Associates S-600 spectrometer. This spectrometer is capable of generating a variety of velocity wave forms suitable for driving the radioactive source through a range of Doppler velocities. In particular, use of the offset mode permitted a single Mössbauer absorption peak to be recorded with high accuracy. The γ-ray source (Amersham Co., initial activity 100 mCi) consisted of ^{57}Co diffused into a 6-μm rhodium foil. The transmitted γ rays were detected by a conventional gas-filled proportional counter. The detector output was amplified and shaped with Canberra and Nuclear Data electronics, while a Nuclear Data 2200 multichannel analyzer was used for data accumulation. Spectrum fitting was accomplished using either Lorentzian profiles (whole spectrum analysis) or a smoothed cubic spline fit (single peak monitoring). Values of the isomer shift (δ), quadrupole splitting (E_Q) and hyperfine field were calculated from the Lorentzian profiles after calibration with a natural iron foil.

III. RESULTS

The room-temperature Mössbauer spectrum of the iron catalyst after carburization is shown in Fig. 4, with the corresponding parameters given in Table 1. The spectrum, obtained in air after the sample had been removed from the *in-situ* reactor cell, exhibits a single six-line magnetically split

TABLE 1

Mössbauer Parameters for Room-Temperature Iron Catalyst after Carburization

Component	δ (mm/sec)	E_Q (mm/sec)	H (kOe)	Area fraction
ε'-Carbide	0.26	0.07	171	0.63
Superparamagnetic carbide/oxide				0.37

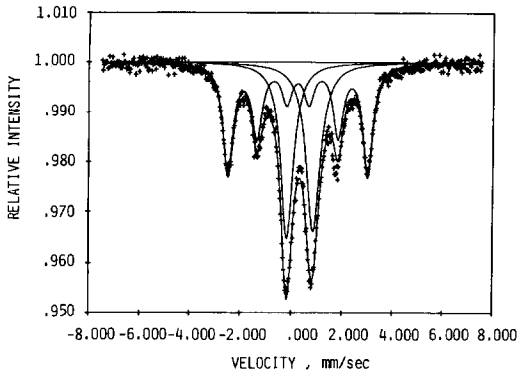

FIG. 4. Room-temperature Mössbauer spectrum of the iron catalyst after carburization. Crosses = experimental data; solid lines = computer fit of spectrum.

pattern with a superimposed doublet. The hyperfine field of the six-line spectrum is 171 kOe; this is in good agreement with the published value of 173 kOe for the ε'-iron carbide (*15, 16*). No other carbides can be detected from the Mössbauer spectrum. The central doublet can be attributed to either superparamagnetic carbide or a passivation product caused by exposure to air (*15, 23*). The critical feature to note from Fig. 4, however, is that the only initial carbide formed from the supported iron catalyst was the ε'-carbide.

Since the primary goal of this work was to use the hyperfine field of the iron carbide crystallites as an "internal thermometer" during the catalytic reaction, it was considered desirable to distinguish the microscopic temperature of the crystallites from the macroscopic temperature of the bulk catalyst wafer. This was accomplished by introducing a thermocouple into the *in-situ* reactor through the gas inlet line. The tip of this monitor thermocouple was placed in direct contact with the catalyst wafer so that its temperature could be measured while a Mössbauer spectrum was being recorded. Table 2 lists the nominal temperature of the cell (measured by the control thermocouple embedded in the copper cell body) and the actual bulk wafer temperature measured by the monitor thermocouple under both the $3H_2/CO$ reaction mixture and helium. The results in Table 2 indicate that the actual temperature of the catalyst wafer was 25 to 30°C higher than the temperature measured by the control thermocouple in the body of the *in-situ* cell. The most probable cause of this temperature difference is nonuniformity in the heat output of the cartridge heaters along their length. Regardless of the origin of the temperature difference, the monitor thermocouple indicated that the catalyst temperature remained stable during these experiments. As mentioned in Section II, the monitor thermocouple recorded temperature fluctuations of less than 0.25°C during a typical 2- to 3-h data acquisition period.

A surprising result shown in Table 2 is that the catalyst wafer was actually hotter under an inert atmosphere than it was when the reaction mixture was in the *in-situ* cell. It is believed that this effect arose from the slightly higher thermal conductivity of helium relative to a 3 : 1 mixture of hydrogen and carbon monoxide.

One result of the measurement of a true higher bulk wafer temperature is that the expected magnitude of the hyperfine field is reduced. This effect was indeed observed when Mössbauer data were acquired under reaction conditions. Figure 5 illustrates the Mössbauer spectrum that was obtained from the iron catalyst in the *in-situ* cell at 250°C. The computer fit of the spectrum features a single hyperfine field with several broad peaks in the center of the spectrum. The linewidth of the hyperfine field in Fig. 5

TABLE 2

Measured Bulk Catalyst Temperatures

Nominal cell temperature (°C)	Catalyst bulk temperature (°C)	
	$3H_2/CO$	Helium
250	277	279
275	299	303
300	329	332

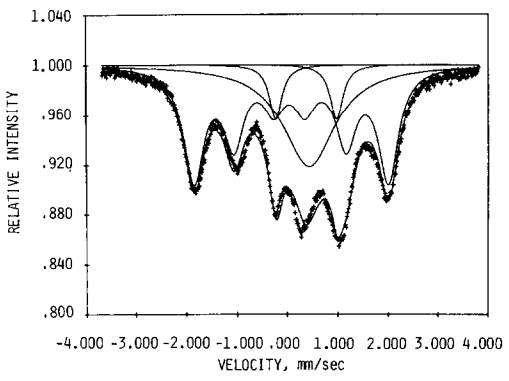

FIG. 5. Mössbauer spectrum of the iron catalyst obtained in the *in-situ* cell under reaction conditions (250°C, $3H_2/CO$ atmosphere). Crosses = experimental data; solid lines = computer fit of spectrum.

was virtually identical to that in the room-temperature Mössbauer spectrum, thus indicating that temperature gradients within the catalyst wafer were negligible. The strength of the hyperfine field for the catalyst under reaction conditions was 120 kOe. If the hyperfine field of the iron carbide crystallites followed the conventional temperature dependence of saturation magnetization as given by Eq. (1), then insertion of the appropriate values for the ε'-carbide along with the actual wafer temperature of 277°C would yield an expected magnetic field of 132 kOe. It is believed that uncertainties in the experimental determinations of the Curie temperature of the ε'-iron carbide (*19*) probably account for the discrepancy between the observed and calculated values for the hyperfine field strength.

Because of its increased sensitivity to the positions of the outer peaks in a magnetically split Mössbauer spectrum, the offset mode of spectrometer operation was employed to monitor peak position during reaction gas/inert gas cycling. Figure 6 shows two pairs of absorption peaks that were obtained at ambient temperatures of 275 and 300°C. The figure clearly indicates that the absorption peaks shift toward lower Doppler velocities (smaller channel number) when the gas flow is switched from helium to the $3H_2/CO$ reaction mixture. At ambient temperatures of 250°C and below no peak shift towards lower velocities was observed under reaction conditions.

The higher temperature of the catalyst wafer under flowing helium supports the validity of the Mössbauer temperature measurements for characterization of the microscopic temperature rise of the supported crystallites. If the changes in the internal magnetic field arose from the influences of the bulk catalyst system on the supported iron crystallites then the shift in the absorption peak positions would be the opposite of those observed experimentally.

During data collection it was found to be most convenient first to collect a spectrum under reaction conditions, and then flush the cell with helium and collect the second spectrum in the inert environment. It was found, however, that the order of the gases

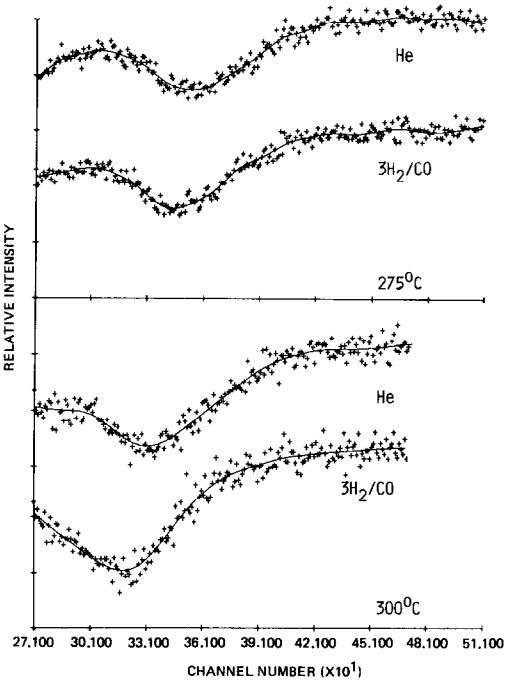

FIG. 6. Mössbauer absorption peaks obtained at 275 and 300°C from iron catalyst under reaction conditions using the offset mode of spectrometer operation. Crosses = experimental data; solid lines = computer fit with smoothed cubic spline.

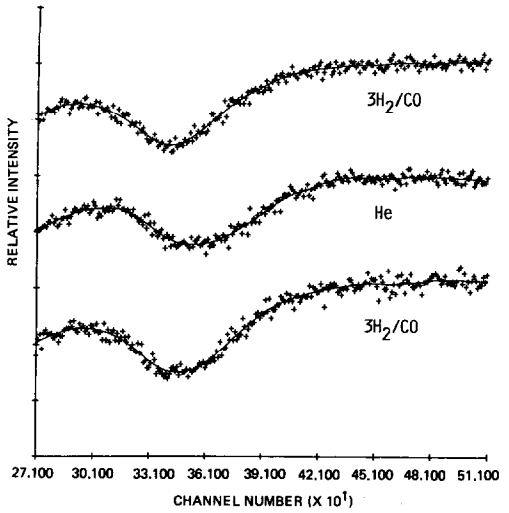

FIG. 7. Effect of gas cycling on Mössbauer absorption peaks at 275°C. Upper peak recorded under reaction conditions ($3H_2/CO$ ambient), middle peak recorded immediately afterwards under helium; bottom peak recorded after reintroduction of $3H_2/CO$. Arrows denote peak mimima determimed from smoothed cubic spline fits.

was not important in the observation of the peak shift. Figure 7 illustrates the result of cycling from the reaction mixture to helium and back to the reaction mixture at 275°C. The figure shows that the decrease in the hyperfine field occurs under reaction conditions regardless of the order that the gases were introduced.

Table 3 lists the magnitude of the shifts in the ε'-carbide absorption peaks during cycling between the $3H_2/CO$ reaction mixture and helium. The peak shifts are given in terms of multichannel analyzer channels as well as the corresponding change in the hyperfine splitting in millimeters per second and in kiloOersteds. The temperature differences ΔT were calculated from a calibration curve of the internal magnetic field versus the measured catalyst bulk temperature. This temperature calibration was obtained by recording several carbide absorption patterns as a function of bulk temperature under flowing helium. It is estimated that the temperature changes are accurate to ±2°C, corresponding to an uncertainty in the change in the hyperfine field of approximately 1 kOe.

The results in Table 3 demonstrate that the temperature of the iron carbide crystallites increased when the gas mixture was switched from helium to $3H_2/CO$. Specifically, temperature increases of the supported iron carbide crystallites of 13 and 19°C were recorded at respective bulk nominal temperatures of 275 and 300°C. Since these temperature measurements were calculated solely from the strength of the internal magnetic field of the iron carbide crystallites, they suggest that the local temperature of the supported particles increased significantly above the ambient temperature under reaction conditions.

It was mentioned above that the calibration curve of the carbide hyperfine field as a function of bulk temperature was obtained under flowing helium. One unexpected result of this calibration was the observation of a time-dependent change in the carbide absorption peaks at temperatures above 250°C. Figure 8 shows the changes in the outer absorption peaks as the bulk temperature of the catalyst was increased with time under flowing helium. The time on stream of the catalyst at the conclusion of spectrum acquisition is indicated along with the temperature. The figure illustrates that the Mössbauer absorption peaks from the ε'-carbide would decrease in magnitude after several hours at temperatures greater than 250°C under an inert ambient. The disappearance of the absorption peaks became very rapid and hence quite troublesome at temperatures in excess of 300°C. In some

TABLE 3

Absorption Peak Shifts Observed in *in-Situ* Mössbauer Experiments

Nominal cell temperature (°C)	T/T_c	Channels	Peak shift (mm/sec)	ΔH (kOe)	ΔT (°C)
250	0.761	0	0	0	0
275	0.797	11	0.079	5.0	13
300	0.837	16	0.115	7.2	19

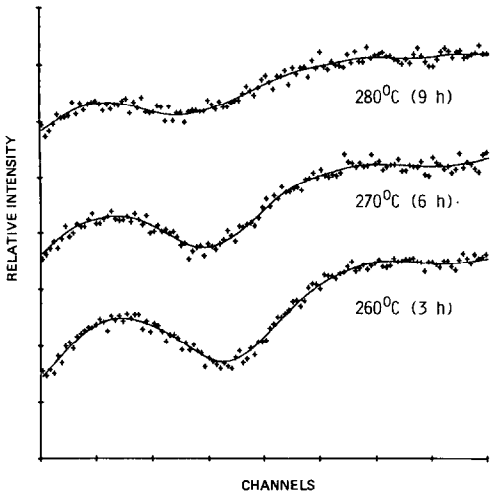

FIG. 8. Changes in Mössbauer absorption peaks of the iron carbide catalyst after prolonged treatment in flowing helium. All peaks were recorded sequentially under helium atmosphere in the *in-situ* cell. Bottom peak recorded at 260°C (3 h under helium), middle peak recorded at 270°C (6 h under helium), top peak recorded at 280°C (9 h under helium).

experiments performed above 300°C, the carbide absorption peaks would disappear completely within 1 h.

Initially it was believed that the disappearance of the carbide peaks was due to a decarburization process. Removal of carbon from the iron carbide would leave behind iron metal, however, and the Mössbauer spectrum of the metal should have been observed. No such metallic spectrum was present. It was found instead that the ε'-carbide transformed into the χ-carbide structure during the helium treatment. Figure 9 shows the room-temperature Mössbauer spectrum of the catalyst wafer after it had been treated in helium at 300°C in the *in-situ* cell. The spectral parameters listed in Table 4 are very similar to those of the χ-carbide (*16*). Also, the relative intensities of the magnetically split components in Fig. 9 are similar to those reported by Raupp and Delgass (*16*) for χ-carbide supported on Cab-O-Sil EH5. The Curie temperature of the χ-iron carbide is approximately 250°C, so no magnetically split spectrum would be present at elevated temperatures under helium after the ε'- to χ-carbide transformation had taken place.

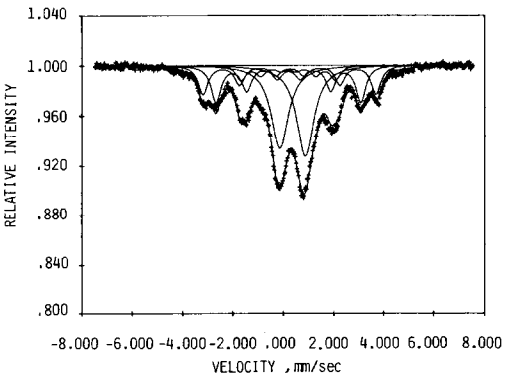

FIG. 9. Room-temperature Mössbauer spectrum of the supported iron carbide catalyst after treatment in helium at 300°C in the *in-situ* reaction cell.

TABLE 4

Mössbauer Parameters for Iron Catalyst after Treatment in Helium at 300°C

Component	δ (mm/sec)	E_Q (mm/sec)	H (kOe)	Area fraction
χ-Fe_5C_2 I	0.21	0.0	179	0.23
χ-Fe_5C_2 II	0.26	0.0	213	0.18
χ-Fe_5C_2 III	0.20	0.0	116	0.09
Superparamagnetic carbide				0.49

IV. DISCUSSION

The experimental findings reported in the previous section suggest that the temperature of the iron carbide crystallites responsible for the Fischer–Tropsch synthesis does indeed increase above the measured ambient temperature during the reaction. These results thus appear to contradict the findings of Holstein and Boudart (*9*), while supporting those of Luss (*5*), Chan *et al.* (*6*), and Steinbrüchel and Schmidt (*8*). However, in order to accept these measurements as being indicative of local temperature increases, it is necessary to judge the magnitude of any macroscopic thermal effects that might have accompanied the re-

action. This was accomplished by estimating both the amount of heat liberated during the synthesis reaction and the heat transfer properties of the catalyst itself. A measure of the catalyst activity was obtained by connecting the *in-situ* reactor cell to a gas-handling and analysis system that has been described in detail elsewhere (*24*). An analysis of the products of the synthesis reaction showed that the turnover frequency (measured as the number of CO molecules reacted per surface iron atom per second) decreased from 5×10^{-3} (site-sec)$^{-1}$ at 1% conversion to 1×10^{-3} (site-sec)$^{-1}$ at 6% conversion. The decrease in specific activity with increasing conversion has been observed in iron catalysts previously (*15, 24*). It must be stressed that the values of specific activity should be viewed as order-of-magnitude estimates only, since the geometry of the *in-situ* Mössbauer cell and the presence of the catalyst as a compressed wafer precluded any rigorous characterization of catalyst performance. Using these reaction rates, it is possible to estimate the magnitude of thermal or concentration effects using the well-known relations (*25*) for intrapellet diffusion and thermal gradients. Calculations using the appropriate relationships for heat and mass transfer in a porous catalyst have demonstrated (*20*) that the rate of reaction is exceeded by the rate of diffusion by at least six-orders of magnitude, and that the catalyst system is at least three orders of magnitude below the level where thermal gradients might occur.

In addition to estimating the thermal effects within the bulk wafer during the reactions, it is possible to approximate the local temperature rise in the supported crystallites that would be expected from the model of Luss (*5*). That model predicts that the maximum temperature increase in supported crystallites would be given by

$$\theta' = ql/kt \tag{2}$$

for small crystallites, and

$$\theta'' = 2q\sqrt{l/\pi\rho ckt} \tag{3}$$

for larger crystallites. In these equations, q is the heat released by a single reacting molecule during the time t, while k, c, ρ, and l are the thermal conductivity, heat capacity, density, and thickness, respectively, of the supported crystallites. Unfortunately, the rigorous application of Luss's model to the supported iron carbide catalyst is hindered by our lack of knowledge of precise values for the parameters in the above equations. Nevertheless, one can use thermal data from bulk iron carbides (*26*) in conjunction with the values of q and t given by Luss (*5*) for a platinum catalyst to obtain an estimate of the temperature rise anticipated during the reaction. Substitution of the appropriate values into Eq. (3) yields a maximum temperature rise for a supported Fischer–Tropsch catalyst of 473°K. Although the precise value of this temperature increase should certainly be viewed with reservation, it indicates that the model developed by Luss would predict large temperature rises during the Fischer–Tropsch reaction over the carbide crystallites. It seems doubtful that the iron carbide crystallite structure could survive temperature rises of several hundreds of degrees. Nonetheless, this model illustrates that while the macroscopic temperature of a Fischer–Tropsch catalyst might remain stable during the reaction, the microscopic temperature at the surface of the iron carbide crystallites could increase to a much higher level than would be anticipated from bulk measurements.

At this time it should be stressed that the local temperature rise models of Luss and Chan *et al.* are concerned exclusively with the surface temperature of the catalyst crystallites. In contrast, the shifts in the absorption peaks recorded during the *in-situ* Mössbauer experiments are indicative of the bulk temperature of the iron carbide particles. Although it is not the purpose of this paper to elucidate the exact distinction between bulk and surface temperatures, it seems safe to assume that an increase in the temperature at the surface of a crystallite would result in either no change or a corre-

sponding temperature increase in the crystallite interior. Therefore, a temperature increase calculated from a model similar to Luss' should be viewed as an upper bound to the possible temperature in the bulk crystal. There are several factors that could result in a reduction in the final bulk temperature following a large increase in surface temperature. For instance, Kember and Sheppard (*14*) were able to monitor the increase in temperature of a nickel catalyst during oxidation using an infrared technique. Therefore, it is likely that radiative heat transfer could cause the surface temperature to decrease and would hence reduce the final bulk temperature. A different mechanism for the reduction of the surface temperature of the crystallites might be found in the desorption of reactant molecules from the crystal surface. Since the adsorption of the reactants in the Fischer–Tropsch reaction is a thermally-activated process (*24*), an increase in the temperature of the surface would enhance the desorption rate of the previously chemisorbed molecules. The endothermic process of desorption would thus tend to lower the surface temperature immediately following the release of the heat of reaction and would contribute to a reduction of the heating of the bulk crystal. Therefore, the discrepancy between the temperature rise predicted by Luss' model and the rise observed in the *in-situ* Mössbauer experiments can at least partially be attributed to processes such as radiative emission and endothermic desorption of reactants.

The local temperature rise models of Luss, Chan *et al.*, and Steinbrüchel and Schmidt all predict that the size of the supported catalyst crystallite should have an impact on the magnitude of the temperature effect. As mentioned in Section II, the particle size distribution of the iron carbide catalysts used in this study was found to be very broad with a number average particle size of 5.2 nm. It would therefore be reasonable to expect that the different sized crystallites should exhibit a variety of temperature increases. In terms of the *in-situ* Mössbauer experiment, this heterogeneity in crystallite temperature would be reflected in an asymmetric broadening toward lower Doppler velocities. The experimental results showed instead a homogeneous peak shift as the gas ambient was switched from helium to the $3H_2/CO$ reaction mixture. Although a precise analysis of peak shape proved difficult because of the low transmitted intensities and consequent poor γ-ray counting statistics, an examination of the first derivative of the spline fit to the data indicated that the absorption peaks were actually slightly broader under the inert helium atmosphere. The broadening of the peaks under helium is not surprising, however, since the large time-dependent changes illustrated in Fig. 8 suggest that an appreciable fraction of the ε'-carbide could have transformed to the superparamagnetic χ-carbide during the 3-h spectrum acquisition time. Since Mössbauer absorption peaks are broadened both by the onset of phase transformations and superparamagnetic collapse, it is likely that both factors contributed to the observed lineshape under helium.

The occurrence of a homogeneous absorption peak shift under reaction conditions implies that the temperature increase of all crystallites is the same. This seems at first contradictory to the three models described earlier, however, it is important to note that the *in-situ* Mössbauer experiment is sensitive to only an unknown fraction of the size-distributed iron carbide crystallites in the catalyst. At the small particle end of the distribution (<5 nm), the crystallites would exhibit superparamagnetic behavior at room temperature and above. These small particles, although catalytically active, would show no magnetic splitting and hence would not be observable. On the other hand, the largest crystallites could in fact be the χ-carbide under reaction conditions; Raupp and Delgass (*16*) have reported that the χ-carbide is the preferred

structure formed during the carburization of large supported iron crystals, while smaller crystals tend to transform into the ε- or ε'-carbide. The lower Curie temperature of the χ-carbide compared to that of the ε'-structure (250°C versus 450°C) would render the larger crystallites invisible during the *in-situ* Mössbauer characterization. Therefore, the temperature rise observed during the *in-situ* Mössbauer experiments applies only to the ε'-iron carbide crystallites that occupy a certain narrow "slice" of the particle size distribution. It is likely that crystallites in the size range of 5 to about 7.5 nm would be large enough to avoid superparamagnetic behavior while maintaining the ε'-structure under reaction conditions.

ACKNOWLEDGMENTS

This work was supported by the U.S. Department of Energy under Contract DE-AC02-78ER04993. The X-ray, TEM, and Mössbauer characterizations were performed in the facilities of the Northwestern University Materials Research Center (NSF Contract DMR-8216972).

REFERENCES

1. Hill, C. G., Jr., "Introduction to Chemical Engineering Kinetics and Reactor Design," New York, Wiley, 1977, p. 458.
2. Hughes, R., and Koh, H. P., *Chem. Eng.* **1,** 186 (1970).
3. Kehoe, J. P. G., and Butt, J. B., *AIChE J.* **18,** 347 (1972).
4. Trimm, D. L., Corrie, J., and Holton, R. D., *Chem. Eng. Sci.* **29,** 2009 (1974).
5. Luss, D., *Chem. Eng.* **1,** 311 (1970).
6. Chan, S. H., Low, M. J. D., and Mueller, W. K., *AIChE J.* **17,** 1499 (1971).
7. Ruckenstein, E., and Petty, C. A., *Chem. Eng. Sci.* **27,** 937 (1972).
8. Steinbrüchel, C., and Schmidt, L. D., *Surf. Sci.* **40,** 693 (1973).
9. Holstein, W. L., and Boudart, M., *Lat. Amer. J. Chem. Eng. Appl. Chem.* **13,** 107 (1983).
10. Dagonnier, R., and Nuyts, J., *J. Chem. Phys.* **65,** 2061 (1976).
11. Jensen, K. F., and Ray, W. H., *Chem. Eng. Sci.* **35,** 241 (1980).
12. Lagos, R. E., Sales, B. C., and Suhl, H., *Surf. Sci.* **82,** 525 (1979).
13. Cusamano, J. A., and Low, M. J. D., *J. Catal.* **17,** 98 (1970).
14. Kember, D. R., and Sheppard, N., *J. Chem. Soc. Faraday Trans. 2* **77,** 1309, 1321 (1981).
15. Amelse, J. A., Butt, J. B., and Schwartz, L. H., *J. Phys. Chem.* **82,** 558 (1978).
16. Raupp, G. B., and Delgass, W. N., *J. Catal.* **58,** 337, 348 (1979).
17. Preston, R. S., Hanna, S. S., and Heberle, J., *Phys. Rev.* **128,** 2207 (1962).
18. Cullity, B. D., "Introduction to Magnetic Materials." Addison–Wesley, Reading, Mass., 1972.
19. Maksimov, Y. V., Suzdalev, I. P., Arents, R. A., and Loktev, S. M., *Kinet. Katal.* **15,** 1293 (1974).
20. Matyi, R. J., Ph.D. dissertation, Northwestern University, Evanston, Illinois, 1983 (Available from University Microfilms, Ann Arbor, Mich.)
21. Warren, B. E., *Progr. Metal Phys.* **VIII,** 147 (1959).
22. Goodisman, J., Brumberger, H., and Cupelo, R., *J. Appl. Crystallogr.* **14,** 305 (1981).
23. Niemantsverdreit, J. T., Filpse, C. F. J., van der Kraan, A. M., and van Loef, J. J., *Appl. Surf. Sci.* **10,** 302 (1982).
24. Amelse, J. A., Ph.D. dissertation, Northwestern University, Evanston, Illinois, 1980 (Available from University Microfilms, Ann Arbor, Mich.)
25. Butt, J. B., "Reaction Kinetics and Reactor Design." Prentice–Hall, Englewood Cliffs, N.J., 1980.
26. Touloukian, Y. S. (Ed.), "Thermophysical Properties of High Temperature Solid Materials," Vol. 5. Plenum, New York, 1967.